REHABILITATION OF EARTHQUAKE-DAMAGED AND SEISMIC-DEFICIENT STRUCTURES USING FIBRE-REINFORCED POLYMER (FRP) TECHNOLOGY

Ong Wee Keong

Fyfe Asia Pte Ltd, Singapore
10 Toh Guan Road #03-10 TT International Tradepark Singapore 608838
fyfeasia@singnet.com.sg

ABSTRACT

In earthquake-prone regions, buildings and other structures are designed with seismic considerations in accordance with guidelines from the international code of practice. However, earthquake tremors from such regions can be experienced in neighboring non-earthquake-prone regions. As such there is a growing concern towards the structural integrity of non-seismically designed (NSD) structures in these non-earthquake-prone regions. Due to little or no concern towards such threats, seismic considerations are not required under the building regulations in these regions. The low available ductility and lack of strength of such NSD structures are posting potential threats to public safety in the event of tremors from a neighboring earthquake. The advent of fibre-reinforced polymer (FRP) technology has provided a potential cost-effective solution to address the deficiencies in these structures. This paper shall look into the potential causes of failure in a NSD RC structure subjected to seismic impact and the techniques to rehabilitate these structures using the state-of-the-art FRP technology.

CHAPTER 1 - INTRODUCTION

Understanding the potential structural failures in NSD RC structures due to seismic impact is vital to address the deficiencies in these structures. In the event of an earthquake, there is tremendous amount of energy released which creates major ground movement. The cyclic loading resulted from the ground movement requires structures to be designed and incorporated with proper detailing to enable them to inhibit lap-splice failures in the plastic-hinge regions and also to have sufficient shear capacity to ensure ductile flexural response. Past records on structural failures in structures due to earthquake showed that brittle failures in structural members are common. There are various different types of failures commonly found in earthquake-damaged structures:-

- Shear and flexure cracks in RC beams
- Crushing of concrete in RC columns near upper/lower ends
- Failure of shear reinforcement ties in RC columns leading to buckling of steel longitudinal reinforcements
- Shear failure in columns and walls
- Failure of beam-column joints
- Failure at construction joints
- Failure of staircases
- Sway mechanism in the structural frame
- Complete collapse or sinking of building due to soft storey

Based on an experimental study performed by Beres et al.[1], there are at least seven critical structural details that could be potential causes of failure in a NSD RC structure subjected to an earthquake. The details are as follows:-

1. Cross-sectional area of longitudinal steel reinforcements in RC column is less than 2% of the concrete cross-sectional area.
2. Lapped splices of the longitudinal steel reinforcements in RC column are above the construction joint.
3. Insufficient confinement provided by transverse steel reinforcements.

4. Construction joints above and below the beam-column connection.
5. Discontinuous positive steel reinforcement in the beam.
6. Lack of transverse steel reinforcements in the panel.
7. Weak column-strong beam conditions.

As observed, the most critical member of the structure in these common structural failures is the vertical structural member – the column.

With its many advantages over conventional strengthening techniques, the FRP technology has been identified as a more viable strengthening technique due to its ease of application, performance, overall time and aesthetical considerations. It offers easier, quicker and reliable application and does not cause distress or add weight to the member to be strengthened. It also forms a protective barrier against ingress of detrimental agents such as moisture, oxygen and carbon dioxide, which helps in arresting further carbonation and corrosion in the strengthened member. This research program series have been designated to understand the effectiveness of FRP technology in strengthening of members of NSD RC structures and rehabilitating earthquake-damaged members.

CHAPTER 2 - OBJECTIVES

A series of research programs, initiated by Fyfe Co. LLC USA and partially funded by California Department of Transportation (CALTRANS), focusing on seismic rehabilitation of structural members of NSD RC structures was carried out. The program conducted seismic rehabilitation on RC rectangular and circular columns, RC beam-column junctions and un-reinforced masonry wall against future seismic impact. The aim of this paper is to look into the seismic upgrade of NSD RC structures using FRP composite system to enhance the ductility, flexural and shear capacities of RC columns. The paper will provide an overview of research programs focusing on seismic rehabilitation of RC columns against future seismic impact. The effectiveness of FRP strengthening to seismic-damaged columns after appropriate repair shall also form part of the discussion in this paper. This part of the research program will allow the understanding on the feasibility and technical effectiveness of the fiberglass/epoxy jacket system in a post-earthquake repair scenario.

CHAPTER 3 - RESEARCH METHODOLOGY

3.1 Test Program

The program will look into the effect of seismic impact on the flexural and shear capacities of vertical structural members of NSD RC structures. A total of three (03) rectangular RC shear column test specimens, four (04) circular RC flexural column test specimens and a circular RC shear column will be subjected to cyclic lateral load and displacement input. These specimens will be tested under the flexural and shear test set-up shown in Figure A-1 and Figure A-2 of Appendix A. The details of test specimens and their retrofitting configurations will be elaborated in the following sections of this paper.

3.2 Specification of FRP Composite Materials

The FRP composite system selected for this series of research programs comprises of E-glass and polyaramid is known as the TYFO® Fibrwrap® Composite System. It is comprised of fibres and are stitched bonded by a process that is able to assemble a variety of materials into a single composite material. This composite meets the demands of the construction industry for a lightweight, easily applicable, structurally powerful, and reasonably priced retrofit material. This particular system has been thoroughly tested worldwide and conforms to ICBO AC125[2]'s, ICBO material characterization, stringent system testing and durability requirements.

The properties of any composite are governed by the individual properties of the constituents. In particular, the properties of the unidirectional FRP are substantially higher in the longitudinal direction than in the transverse direction. It is the longitudinal properties of composites that are mentioned in this literature for comparative

purposes. Properties of the E-glass/Polyaramid composite system used in this research are summarized in Table-1 below.

Table-1: Properties of the E-glass/Polyaramid Composite System

Tensile Strength (MPa)	Elastic Modulus (GPa)	Coefficient of Thermal Expansion (10^{-6}/°C)	Ultimate Strain (%)
575 (typ. test value)	26.1	7.74	2.2

CHAPTER 4 - SEISMIC RESEARCH ON RECTANGULAR RC COLUMNS[3]

Three (03) rectangular RC columns test specimens with clear height of 2.44m (8ft) and a cross-sectional size of 610mm x 406mm (24in x 16in) were fabricated. The columns were reinforced with longitudinal steel reinforcements of diameter 19mm (f_y = 414MPa, Grade 60 #6 bars) to give a longitudinal steel ratio of ρ_L = 0.025. Transverse reinforcements consisted of single peripheral hoops of diameter 6.35mm (#2) plain bars with 90° corner hooks lapped in the cover concrete. The nominal concrete strength at the time of testing was f_c' = 34.5MPa (5000psi). The dimensions and the reinforcement details of the test specimens are shown in Figure A-3 of Appendix A. These columns were identified as RC01, RC02 and RC03 with RC01 as the control specimen and RC02 and RC03 as the FRP composite strengthened specimens subjected to axial compression load of 507kN (114kips) and 1780kN (400kips) respectively. The higher axial compression load for RC03 is to create conditions more critical for confinement. RC02 and RC03 were identically strengthened with 3.42mm thick of the FRP composite over the entire column height and additional 3.42mm thick of the FRP composite over the top and bottom 600mm (2ft) of the columns. It should be noted that all layers were passive. The details of the test specimens are summarized in Table-2 below.

Table-2: Details of Test Specimens – Rectangular RC Columns

S/N	Speci-men	Size (mm)	Rebar (mm)	Remarks
1.	RC01	B-610 D-406 H-2440	22-Ø19(L); Ø6.35-125(T)	Control+ 507kN(V)
2.	RC02			(P)+ 507kN(V)
3.	RC03			(P)+ 1780kN(V)

B-Breadth; D-Depth: H-Height; (L)-Longitudinal; (T)-Transverse; (P)-Passive Retrofit; (V)-Vertical Load

CHAPTER 5 - SEISMIC RESEARCH ON CIRCULAR RC COLUMNS[4]

A total of four circular RC column test specimens were fabricated with diameter of 610mm (24in) and clear height of 3.66m (12ft). The longitudinal steel reinforcements of diameter 19mm (#6 bars) were provided with transverse steel reinforcements of diameter 6.35mm (#2 bars) at spacing of 125mm (5in). The material strengths were f_y = 315MPa and f_c' = 34.5MPa (5000psi). The dimensions and the reinforcement details of the test specimens are shown in Figure A-3 of Appendix A. The four circular column test specimens were identified as CC01, CC02, CC03 and CC04, having CC01 as the control test specimen and the rest retrofitted differently based on active/passive combinations of fibreglass/epoxy confinement layers. CC02 and CC03 were both actively retrofitted with 2.44mm thick and 1.22mm thick of the FRP composites and were also pressure-grouted to achieve an active confinement stress of 1.72MPa and 0.69MPa respectively over the bottom 1.22m height of the column. In addition, both CC02 and CC03 were passively retrofitted with the FRP composites having a nominal thickness of 3.25mm and over the lower height of 305mm (12in). CC04 was pressure-grouted with cement grout to an active pressure of 1.38MPa. The passive retrofit was the same with that for CC02 and CC03 but 1.38mm thick of FRP composite in the circumferential direction and 0.61mm thick of FRP composite with fibre oriented vertically were provided as the active retrofit over 0.91m height instead of 1.22m

height of the column. The details of the test specimens are summarized in Table-3.

Table-3: Details of Test Specimens – Circular RC Columns

S/N	Speci-men	Size (mm)	Reinforcement (mm)	Remarks
1.	CC01	Ø610	26-Ø19(L); Ø6.35-125(T)	Control
2.	CC02			(A-E)+ (P)
3.	CC03			(A-E)+ (P)
4.	CC04			(A-C)+ (P)

(L)-Longitudinal; (T)-Transverse; (P)-Passive Retrofit; (A-E)-Active Retrofit/Epoxy; (A-C)-Active/Cement

CHAPTER 6 - SEISMIC RESEARCH ON EARTHQUAKE-DAMAGED CIRCULAR RC COLUMN[5]

In this part of the program, a circular RC column test specimen with dimensions and reinforcement details identical to that of the CC-series of test specimens in the above earlier research program was used. The specimen was subjected to fully-reversed increasing cyclic lateral load/displacement input until failure. The failed specimen was repaired with patching, epoxy injection and fibreglass/epoxy jacketing with total thickness of 3.88mm for the full height of the column. The specimen was also subjected to an axial compression load of 1780kN (400kips) in both tests carried out without and with retrofitting.

CHAPTER 7 - RESULTS AND FINDINGS

7.1 Test Results on Seismic Research on Rectangular RC Columns for Shear[3]

Figure B-1 of Appendix B shows the lateral force-deflection curve for the control specimen RC01. The rapid degradation after the shear failure should be noted. The shear failure occurred at a drift ratio (displacement/height) of 1.07%. By comparing with RC01, the performance of the two strengthened columns, RC02 and RC03, was remarkably good, as is apparent from the force-deflection hysteresis loops of Figure B-2 and Figure B-3 in Appendix B.

Strengthened specimen RC02 developed stable flexural ductile response with no signs of distress at ductility levels up to $\mu_\Delta = 4.5$. At $\mu_\Delta = 6.0$, first signs of distress in the plastic hinge regions at top and bottom of the column were noted, with slight bulging of the FRP composite jacket on the compression face, indicating that the concrete cover had spalled inside the jacket, and the incipient reinforcement buckling was occurring. At $\mu_\Delta = 8.0$, the bulging became pronounced, with tearing of the composite jacket at one corner in the bottom hinge region. Significant strength degradation occurred, during the three cycles to $\mu_\Delta = 8.0$, but even after the three cycles, lateral forces resisted exceeded the theoretical flexural strength. At ductility $\mu_\Delta = 10.0$, the composite jacket at the lower hinge tore vertically and horizontally resulting in a complete loss of confinement. Degradation was extremely rapid, with crushing of core concrete and buckling of longitudinal steel reinforcement. In the final cycle, several reinforcements were fractured as a result of the low cycle fatigue associated with alternate bending and strengthening. The maximum shear force sustained by RC02 was 979kN (220ksi) at $\mu_\Delta = 8.0$. This was 32.5% above the nominal flexural strength based on measured material properties. The yield displacement at 14.88mm (0.586in) was about 60% larger than predicted based on flexural deformations alone, indicating the strong influence of shear.

With reference to Figure B-3, RC03 attained a peak load of 1498kN (262.5kips) at $\mu_\Delta = 8.0$ which was 39% above the nominal flexural strength. Similar to RC02, the first sights of distress occurred at $\mu_\Delta = 6.0$ with incipient bulging of the jacket on the compression faces of the top and bottom plastic hinge zones. At ductility $\mu_\Delta = 8.0$, the composite jacket in the upper plastic hinge zone tore, resulting in comparatively rapid strength loss. However, the yield displacement was less than RC02 at 12.45mm (0.49in) despite higher yield force. This is due to the reduced significant of shear as a consequence of the beneficial action of the increased axial compression.

Figure B-4 and Figure B-5 show plots of jacket horizontal strain vs displacement at a height of 686mm (27in) above the base of RC02 and RC03 respectively. This location is just above the region of increase composite thickness and is typically a location of high strain. It will be seen that in both cases peak strains are about $3000x10^{-6}$ and that stable loops are obtained.

Typical strain profiles up the sides of the two columns are shown in Figure B-6 and Figure B-7. In both cases, strains are initially higher near the top and bottom of the columns. But as shear cracking extends into the central region, strains increase to similar levels as those in the plastic hinge regions.

7.2 Test Results on Seismic Research on Circular RC Columns For Flexural[4]

Experimental lateral force-lateral displacement hysteresis curves are shown in Figures C-2, C-3 and C-4 in Appendix C for test specimens CC02, CC03 and CC04 respectively. Each plot includes the theoretical load-deflection envelope based on a nominal concrete compressive strength of f'_c = 34.55MPa (shown as a dashed curve). The ideal strength based on f'_c = 34.55MPa, f_y = 315MPa and ultimate compressive strain of 0.006 and a model for confined concrete is also indicated as V_i.

The response of test specimen CC02, with the highest level of effective confinement, is excellent, with stable hysteresis loops up to the third cycle to displacement ductility levels of μ_Δ = +8.0, -6.0. It will be seen that there is no sign of structural degradation associated with bond failure of the starter bars, apparent for control specimen CC01 (compare with Figure C-1). Its behaviour is very close to that of a steel jacket retrofit column reported by Chai et. al[6]. Strength and stiffness differences between CC02 and steel jacket retrofitted columns appear to be primarily due to differences in concrete compression strength. However, structural degradation with fibreglass/epoxy jacket retrofit did not occur until significantly higher displacement than with equivalent steel jacket columns. This apparent improvement in performance may have been a result of more effective confinement at the base of the column, combined with a spread of plasticity up into the column, resulting from the lower stiffness of the retrofit scheme.

The result of CC03, shown in Figure C-3, is very similar to that of CC02 until displacement of approximately 150mm at $\mu_\Delta = \pm 6.0$ when peak loads at each cycle degrade as a consequence of bond failure. It should be noted, however, that the degradation is very gradual and appears to be stabilizing at $\mu_\Delta = \pm 7.0$. It is felt that this is a consequence of the clamping pressure provided across the failing lap-splice. Although this pressure was insufficient to eliminate eventual bond failure, it resulted in a dependable friction force across the failing lap-splice which resisted movement in both directions of loading. It will be noted that the width of the hysteresis loop, measured in the direction of the load axis, at zero displacement decreases after initiation of the bond failure and results in a reduction to the total energy absorbed per cycle.

Despite the higher effective confining stress of CC04, the force-deflection hysteresis behaviour, as shown in Figure C-4, is very similar to that exhibited by CC03 except that degradation of CC04 after bond slip commenced seems to be more gradual than with CC03, and appears to be stabilizing at a higher force level for CC04. It should be noted that CC04 was taken to higher displacements than CC03.

7.3 Test Results on Seismic Research on Earthquake-Damaged Circular RC Columns[5]

Figure D-1 of Appendix D shows the force-deflection hysteresis behaviour of specimen without any retrofitting. The force-deflection hysteresis behaviour of the failed specimen retrofitted by steel jacket and FRP composite jacket are given in Figure D-2 and D-4. The test results indicated that the initial stiffness of the repaired test specimen was very similar to that of the original as-built column and the load-displacement response of the two columns was almost identical up to the displacement ductility $\mu_\Delta = 2.0$. Thus, the repair measure was effective in restoring the original column stiffness despite

the significant shear damage. The as-built column failed rapidly in shear at $\mu_\Delta = 3.0$ but the repaired specimen sustained the cyclic lateral displacements up to $\mu_\Delta = 10.0$ without any sign of lateral capacity degradation and with very stable hysteresis loops. The displacement at $\mu_\Delta = 10.0$ corresponds to a column drift of 4.9%, which is significantly more than what can be expected under a maximum credible earthquake. At $\mu_\Delta = 10.0$, the test was terminated due to limitations in the displacement capacity of the loading system.

A comparison with an identical damaged column repaired with steel jacket retrofit done in a separate research program is provided by Figure D-5. Both the steel jacket retrofitted column and the FRP retrofitted column exhibited the same improved ductile response. This shows that FRP jacket retrofit is fully effective in improving the seismic behaviour equivalent to that of a well designed steel jacket retrofit.

The complete jacket strains response is provided in Figures D-6 to D-13. Vertical strain profiles depicted in Figures D-6 to D-11 show very low circumferential jacket strains in the mid-height region of the column, indicating the effectiveness of the epoxy injection of the inclined diagonal cracks in preventing cracks from reopening. High circumferential strains up to 0.004 were observed in the column end or plastic hinge regions. The circumferential strains along the column perimeter in the lower end region are depicted in Figures D-12 to D-13, and show a strain distribution along the jacket perimeter which does not indicate clear tendencies toward higher jacket strains along the sides or the generators in the loading direction. In Figure D-12, circumferential jacket strains seems to be concentrated at the compressed toe as a result of confinement requirements while the pull direction suggests a more even circumferential jacket strain distribution. Different damage patterns from the original shear column test can be a possible source for this un-symmetric behaviour.

CHAPTER 8 - CONCLUSIONS

The shear tests on rectangular RC columns retrofitted with passive confinement from FRP jacket showed that shear failure of these shear-deficient columns can be inhibited and will also result in high level of ductility, converting brittle shear failure modes to ductile inelastic flexural deformation modes. This response was partly due to the highly elastic nature of the FRP material. The tests also showed that confinement continued to be provided by the FRP jacket even after the buckling of the longitudinal reinforcement with the increase in the elastic restraint of the FRP jacket as a result of the membrane action developing in the deformed jacket.

From the flexural tests, the failure of lap-splices under cyclic inelastic action can be inhibited with the provision of active confinement from the FRP jacket and epoxy/cement pressure-grout. Active confinement is expected to improve the seismic performance of a column than compared with passive confinement as dilation of the concrete core, which is necessary to activate confinement in a passive retrofit, is not essential in an actively confined retrofit.

The re-test of a failed circular RC shear column repaired with FRP jacket and epoxy injection showed that the employed repair technique was fully effective in restoring the original column stiffness characteristics, in transforming the brittle shear failure mode into a ductile flexural mode and in providing displacement ductility to the systems equal to that observed in a comparative full height jacket retrofitted test column.

Based on the results from the research program, NSD RC structures can be retrofitted to withstand potential seismic impact using FRP technology. The effectiveness of the FRP jacket has made it a viable technique for a post-earthquake structural restoration to seismic-damaged structures.

REFERENCES

1. Beres, A. Pessiki, S. P., White, R. N. and Gergely, P. (1996) "Implications of Experiments on Seismic Behavior of Gravity Load Designed RC Beam-To-Column Connections", Earthquake Spectra, Vol. 12, No. 2, May, pp. 185-198.
2. International Conference of Building Officials (2003) "ICBO Acceptance Criteria for Concrete And Reinforced And Un-reinforced Masonry Strengthening using Fibre-Reinforced Polymer (FRP) Composite Systems", ICBO AC125, June 2003.
3. M. J. N. Priestley and F. Seible (1992) "High Strength Fibre Rectangular Column Shear and No-lap Splice Flexural Tests", SEQAD Consulting Engineers Report for Fyfe Co. LLC..
4. M. J. N. Priestley and F. Seible (1994) "Column Seismic Retrofit using Fibreglass/Epoxy Jackets", SEQAD Consulting Engineers Report for Fyfe Co. LLC..
5. M. J. N. Priestley and F. Seible (1993) "Repair of Shear Column using Fibre Rectangular Column Shear and Epoxy Injection", SEQAD Consulting Engineers Report for Fyfe Co. LLC..
6. Chai, Y. H., M. J. N. Priestley and F.Seible (1991) "Seismic Retrofit of Circular Bridge Columns for Enhanced Flexural Performance", ACI Structural Journal, 88 (5):572-584, Sept./Oct. 1991.

APPENDIX A

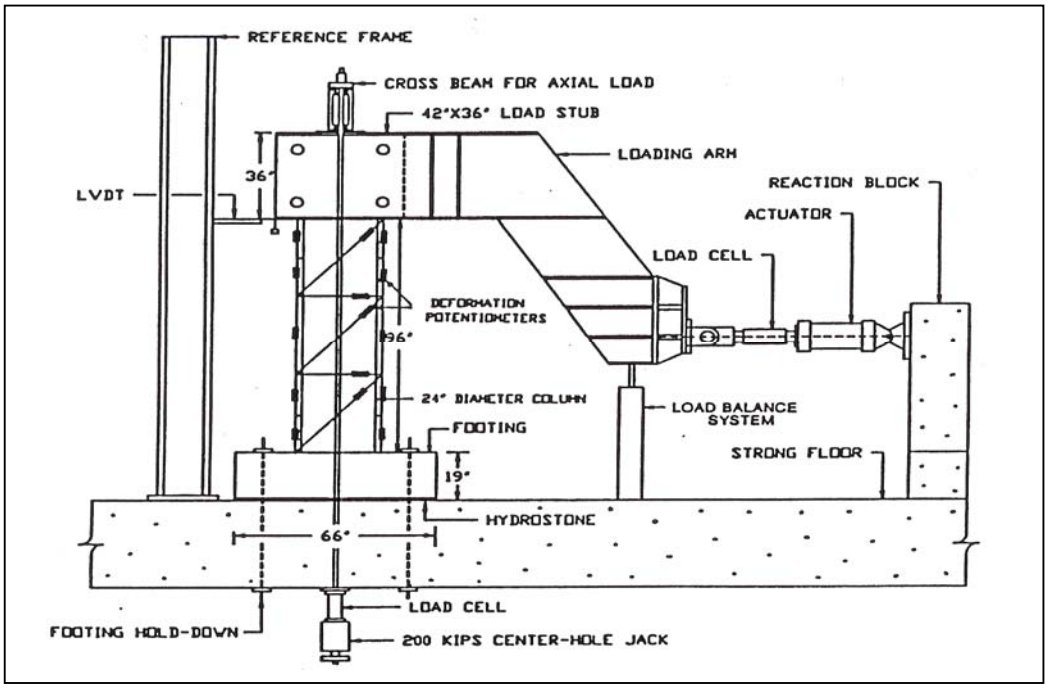

Figure A-1: Test Set-Up for Flexural Test

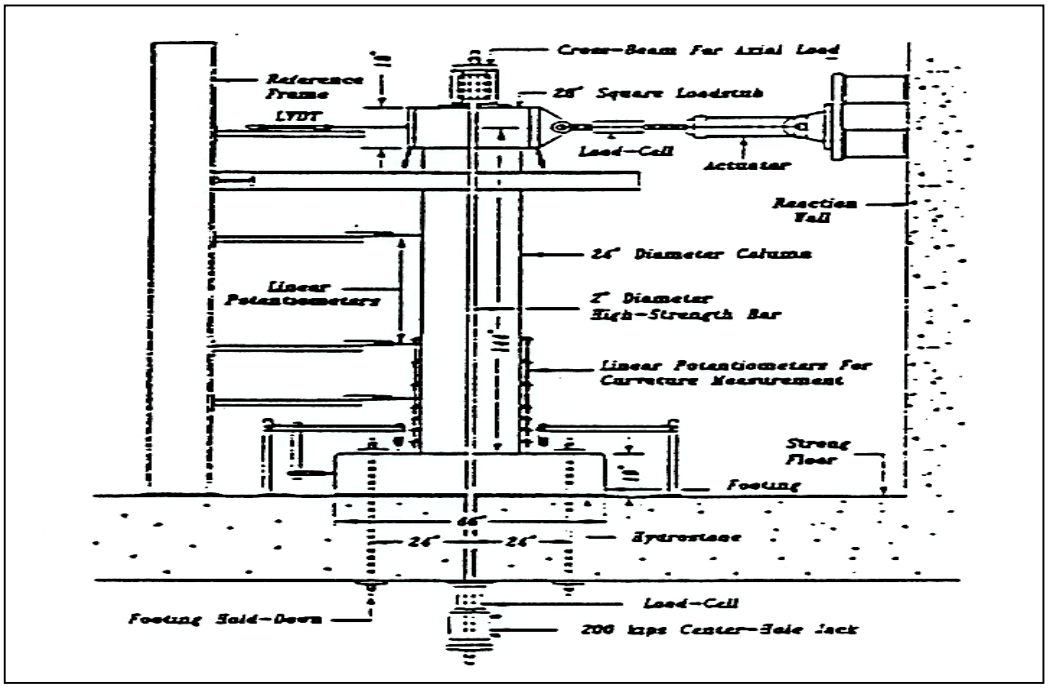

Figure A-2: Test Set-up for Shear Test

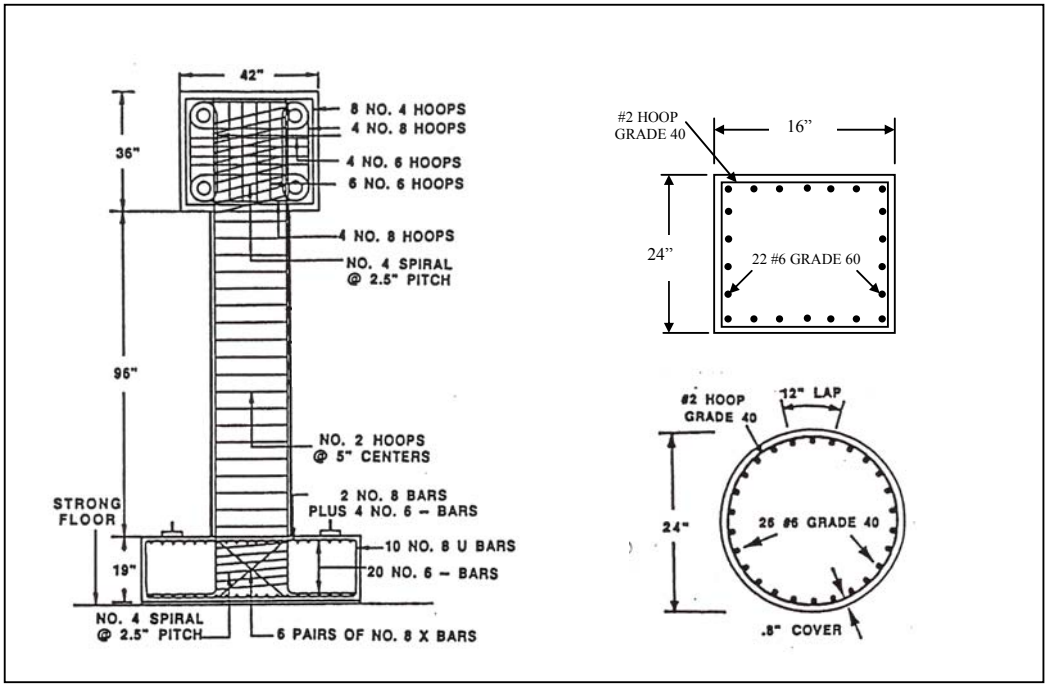

Figure A-3: Dimensions and Reinforcement Details of Test Specimens

APPENDIX B

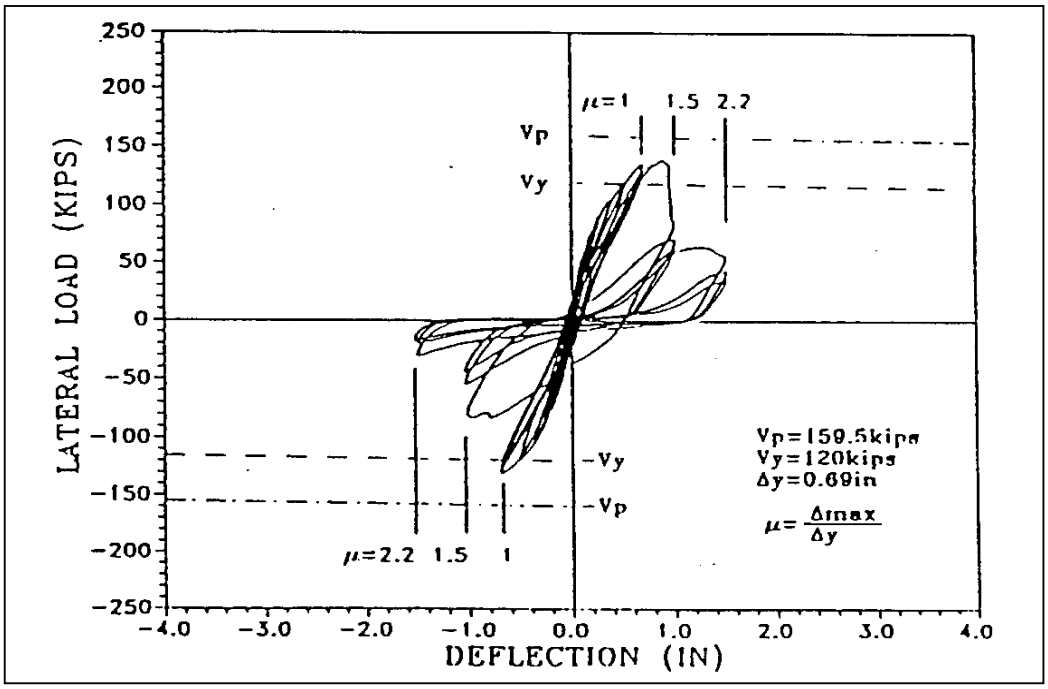

Figure B-1: Hysteresis Loops of Rectangular Column RC01

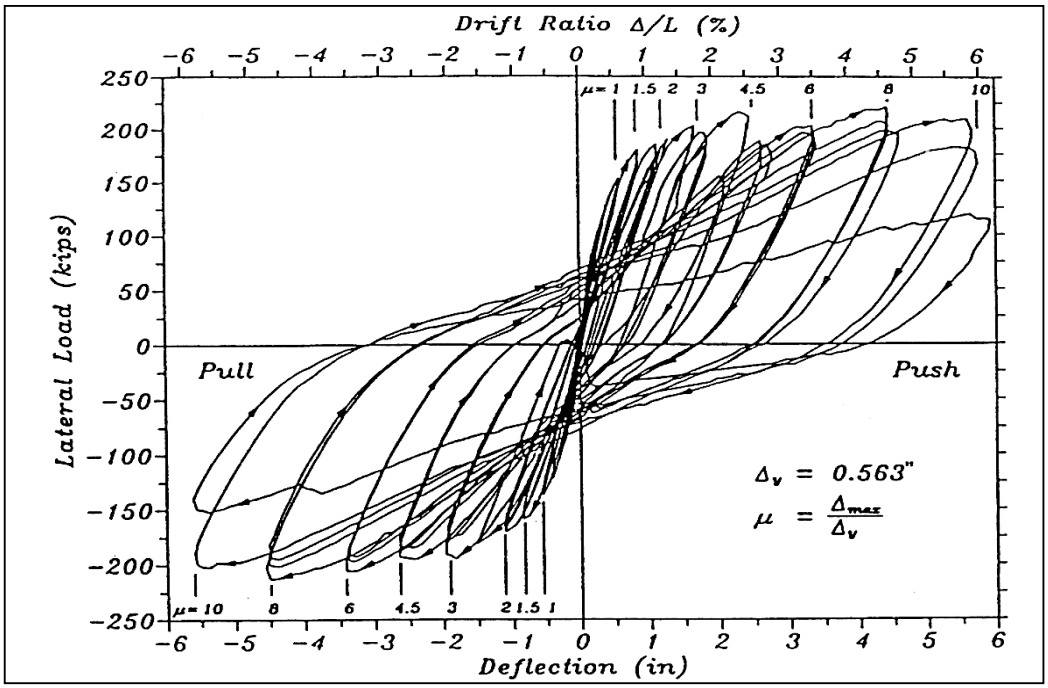

Figure B-2: Hysteresis Loops of Rectangular Column RC02

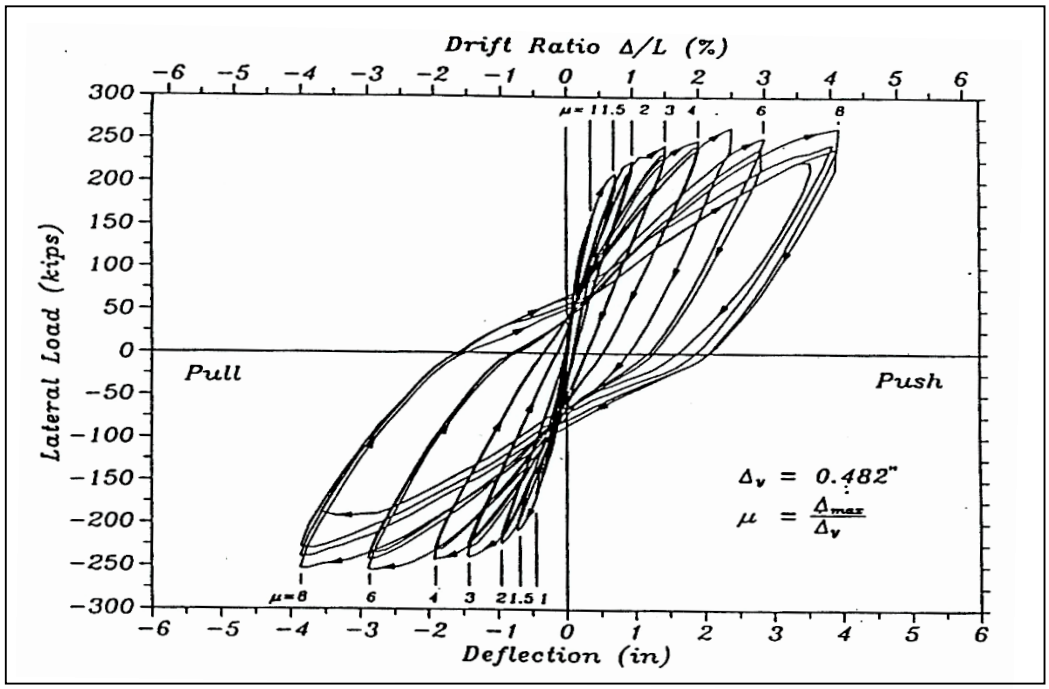

Figure B-3: Hysteresis Loops of Rectangular Column RC03

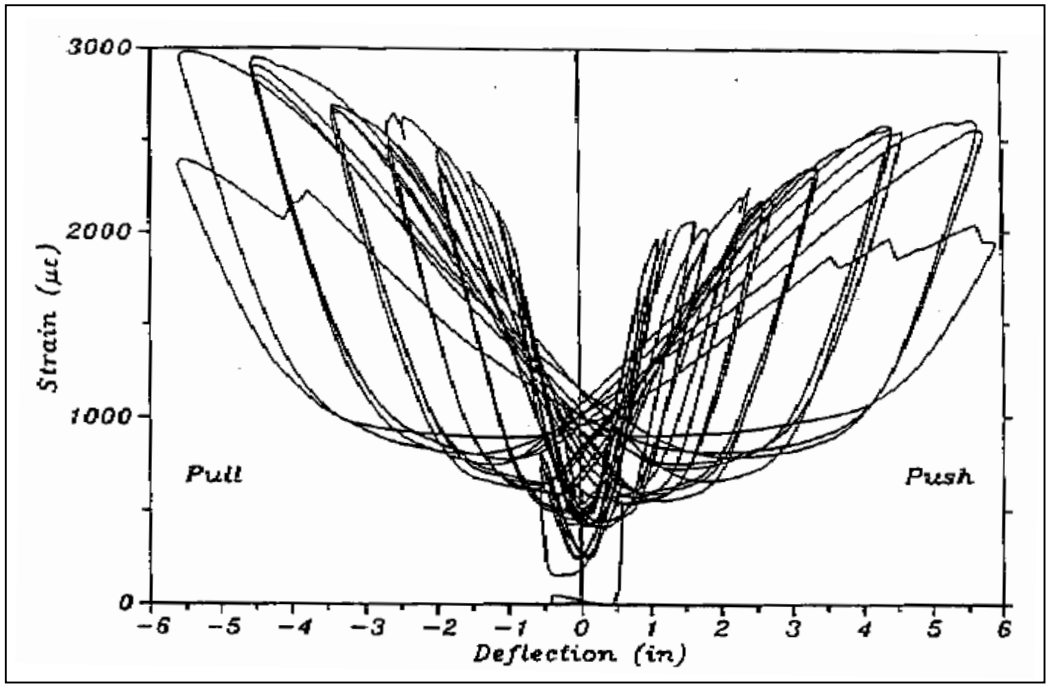

Figure B-4: Typical Strain-Deflection Plots for Rectangular Column RC04

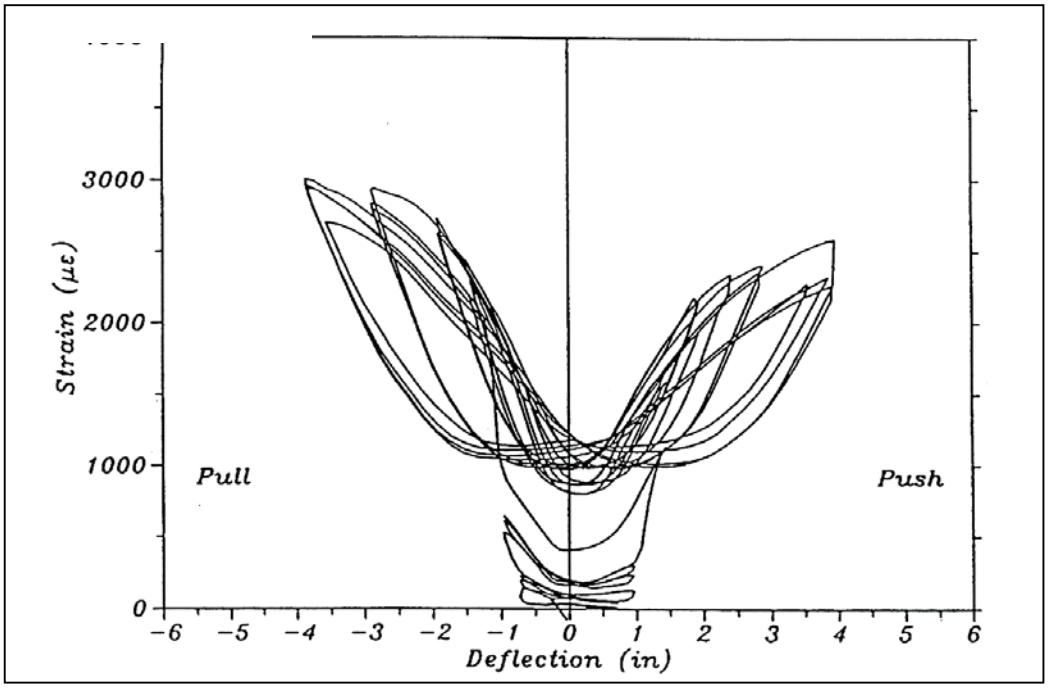

Figure B-5: Typical Strain-Deflection Plots for Rectangular Column RC03

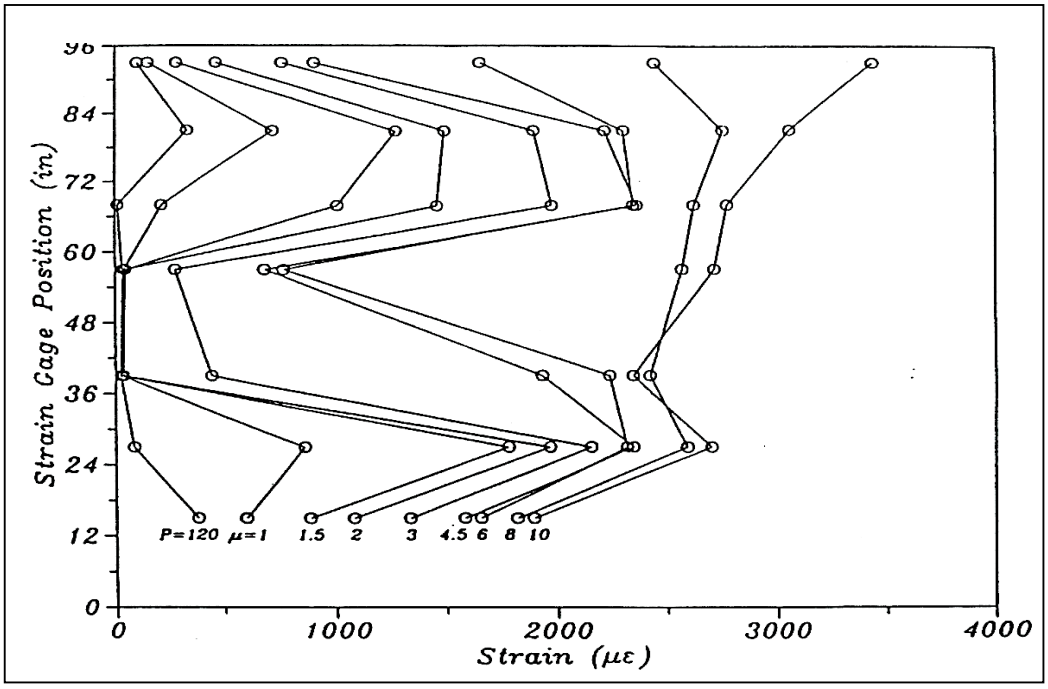

Figure B-6: Typical Strain Profiles at Different Ductilities for Rectangular Column RC02

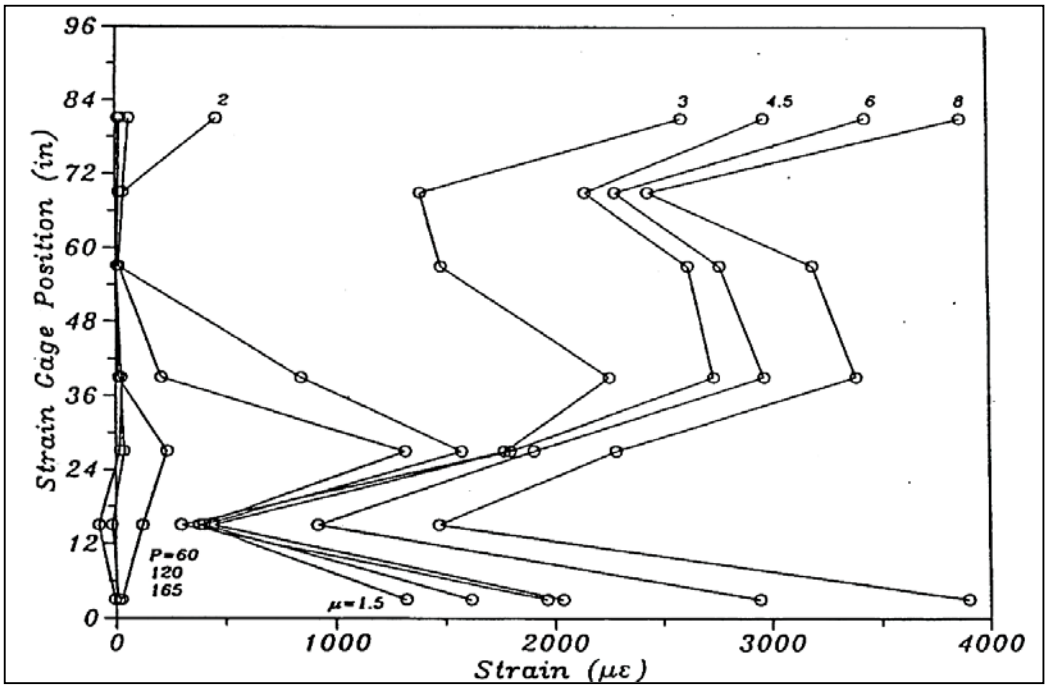

Figure B-7: Typical Strain Profiles at Different Ductilities for Rectangular Column RC03

APPENDIX C

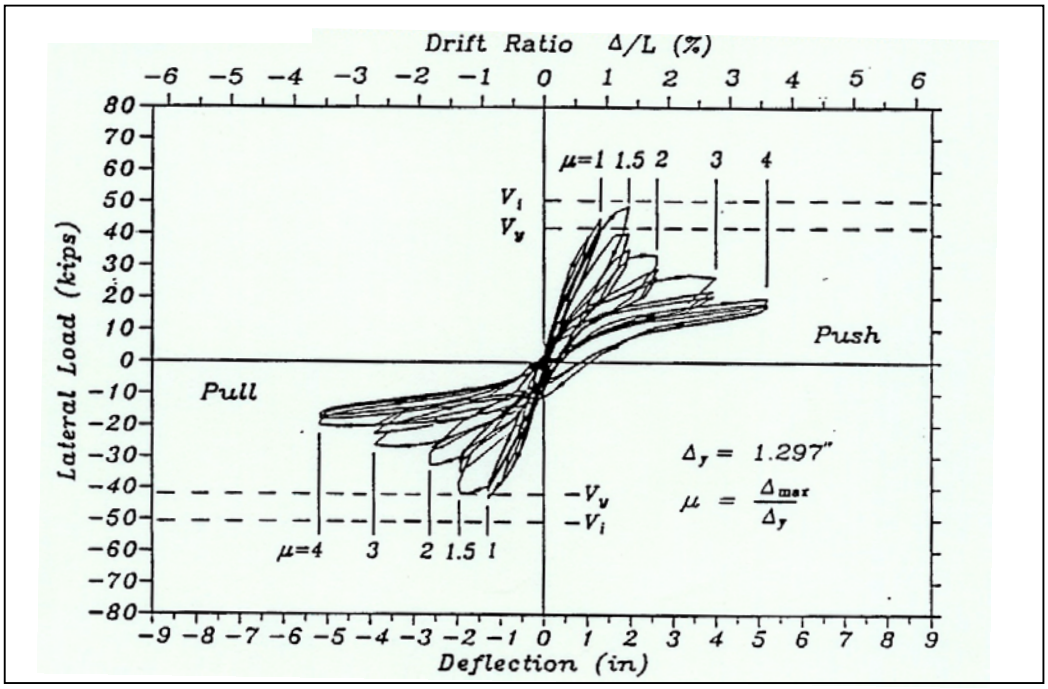

Figure C-1: Hysteresis Loops of Rectangular Column CC01

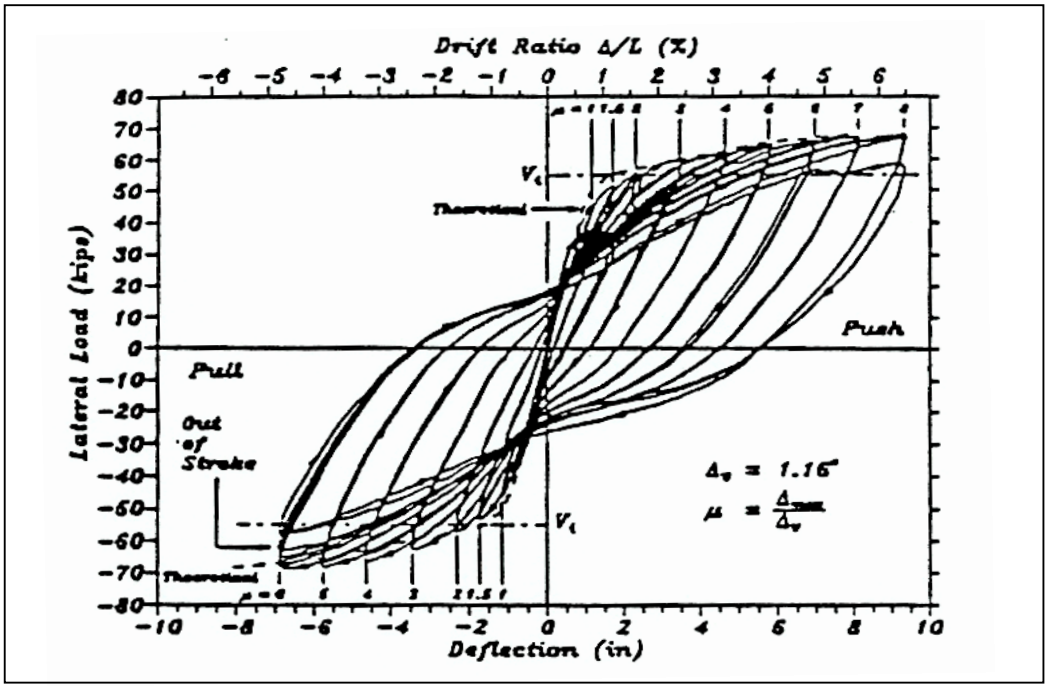

Figure C-2: Hysteresis Loops of Rectangular Column CC02

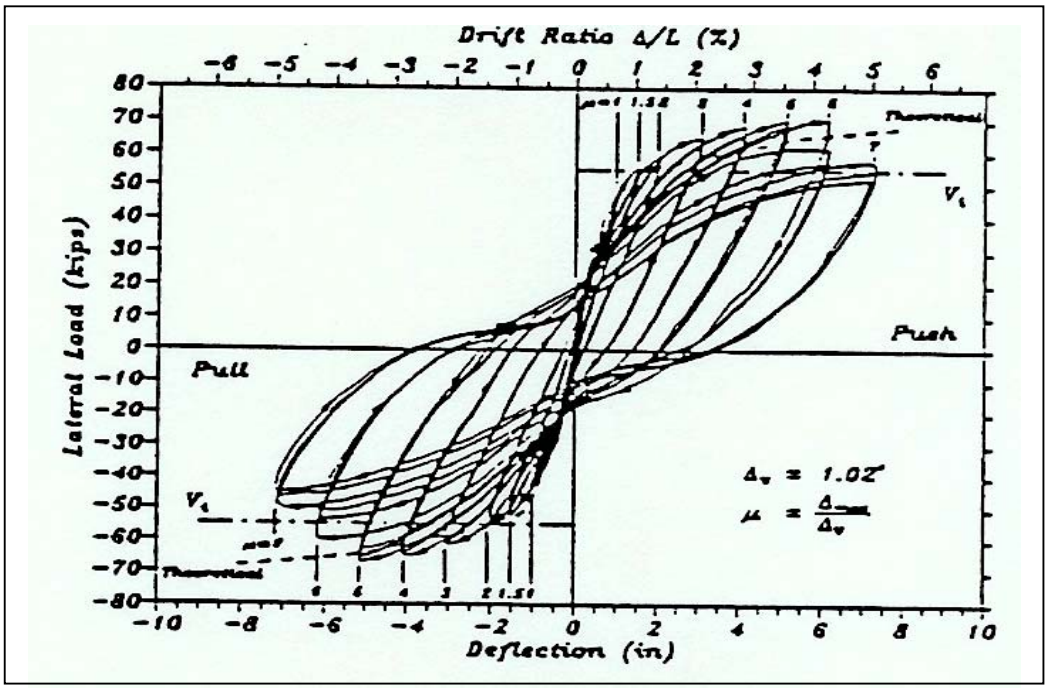

Figure C-3: Hysteresis Loops of Rectangular Column CC03

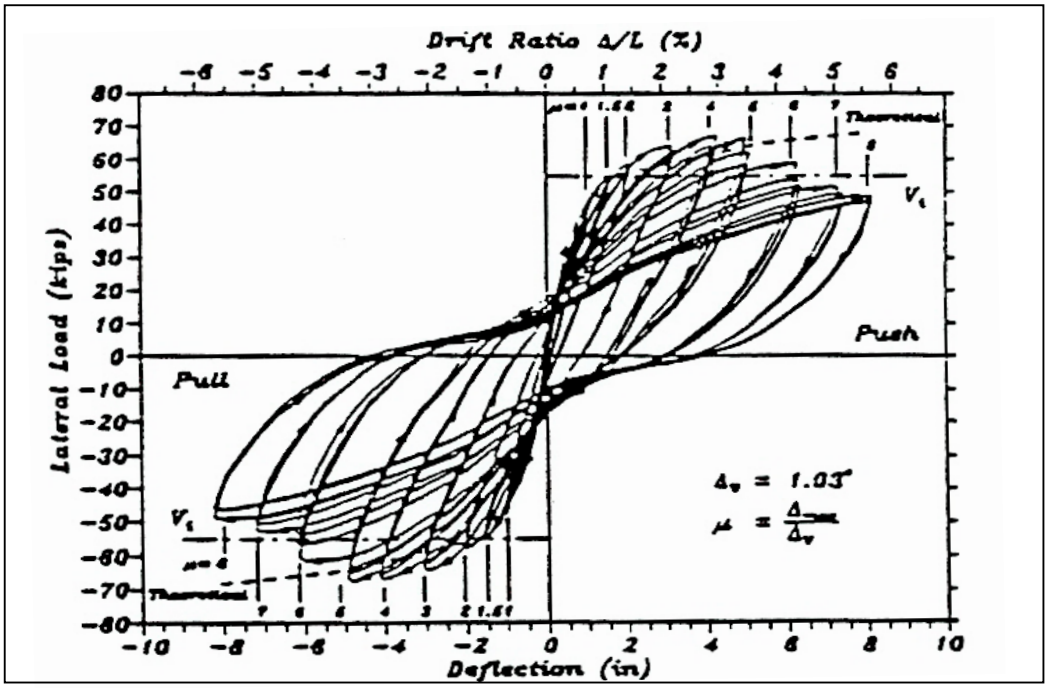

Figure C-4: Hysteresis Loops of Rectangular Column CC04

APPENDIX D

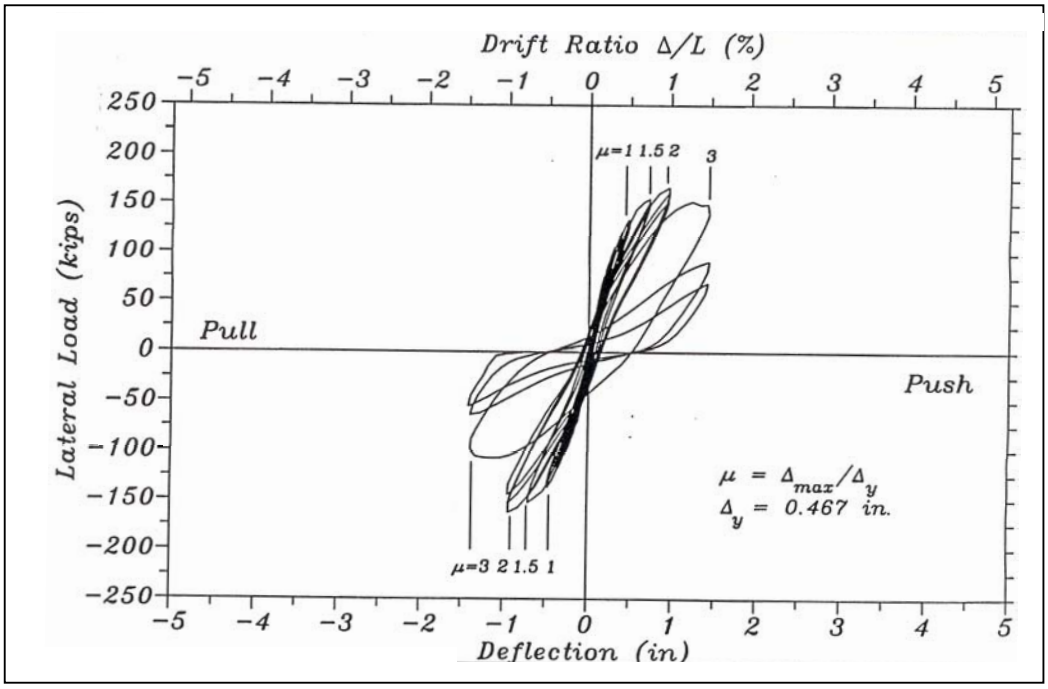

Figure D-1: Hysteresis Loop of Circular Column Before Repair

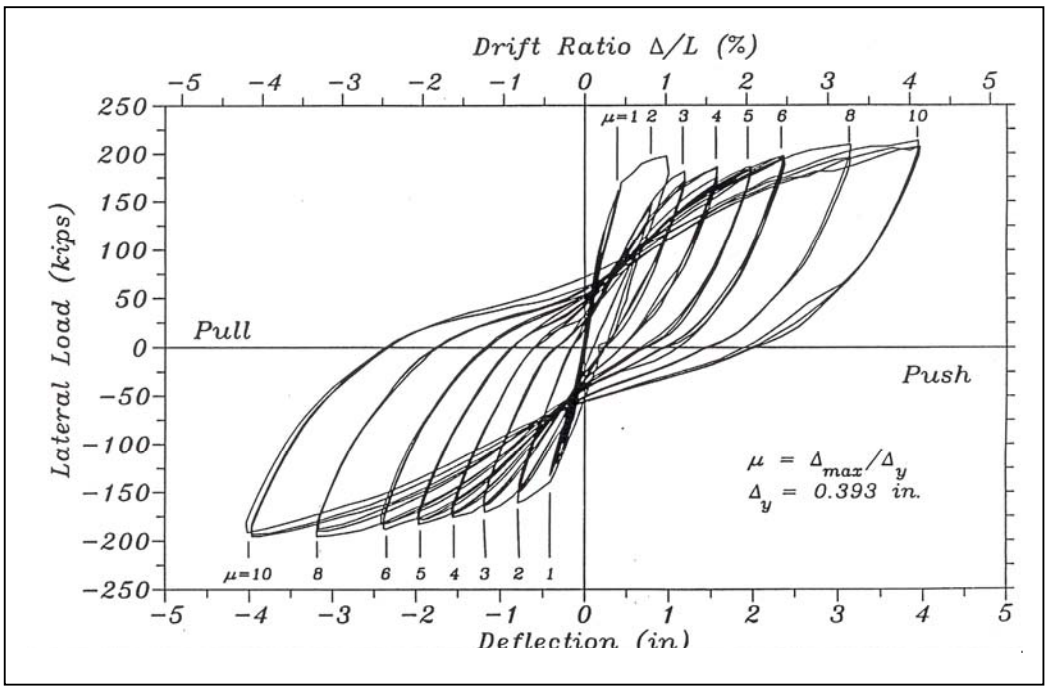

Figure D-2: Hysteresis Loop of Circular Column Retrofitted With Steel Jacket

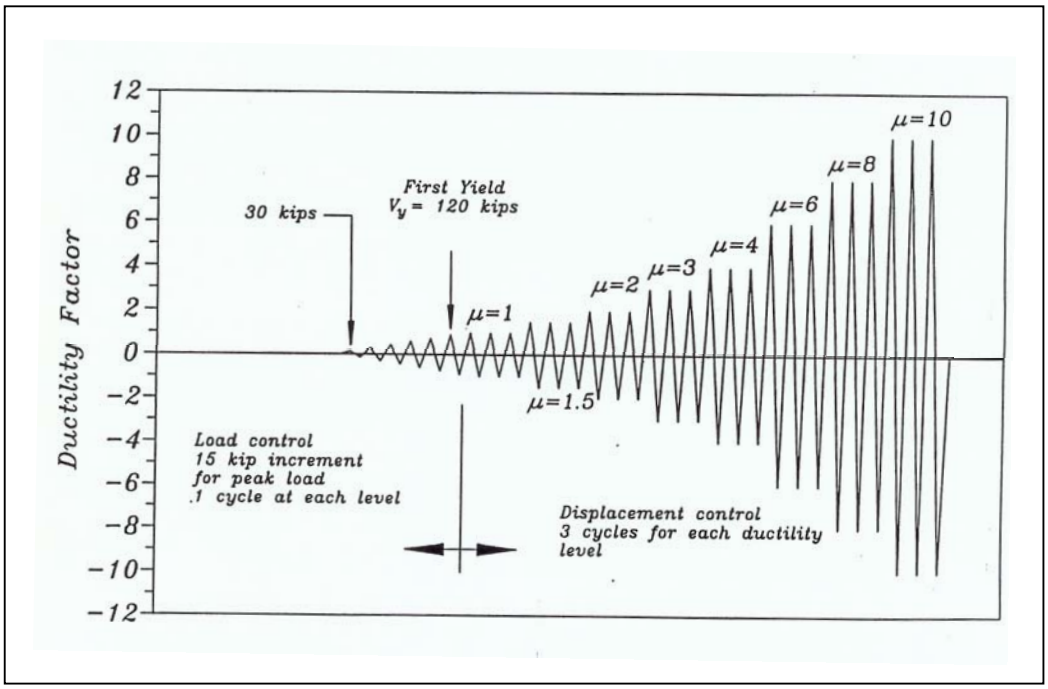

Figure D-3: Loading History

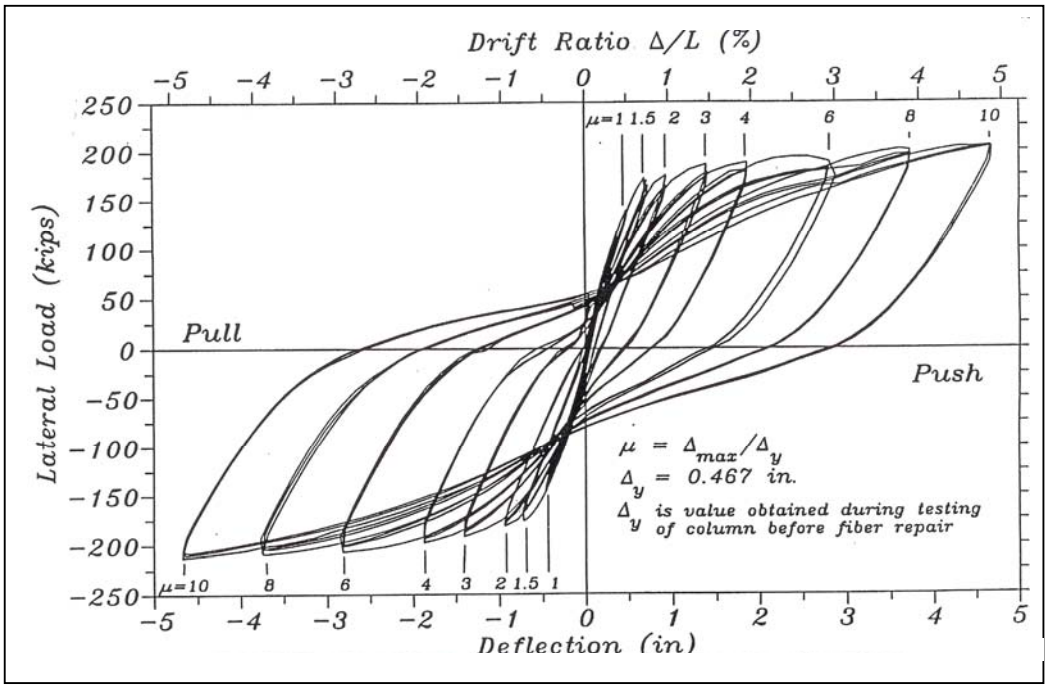

Figure D-4: Hysteresis Loop of Circular Column Retrofitted With FRP Jacket

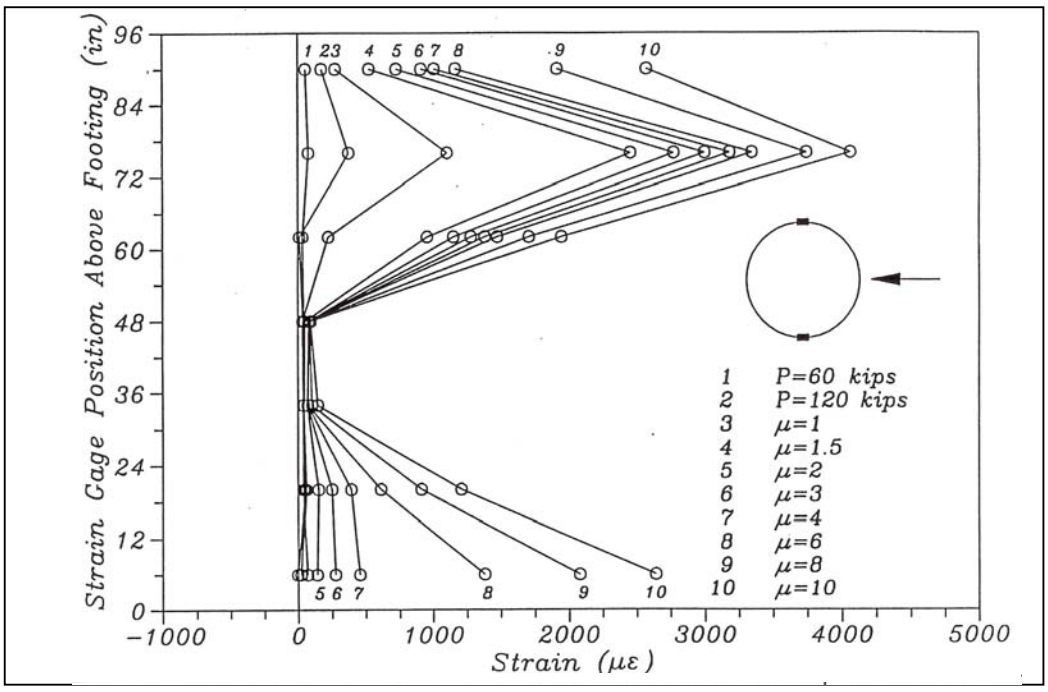

Figure D-6: Strain Profiles for Average of East and West Sides Push Direction

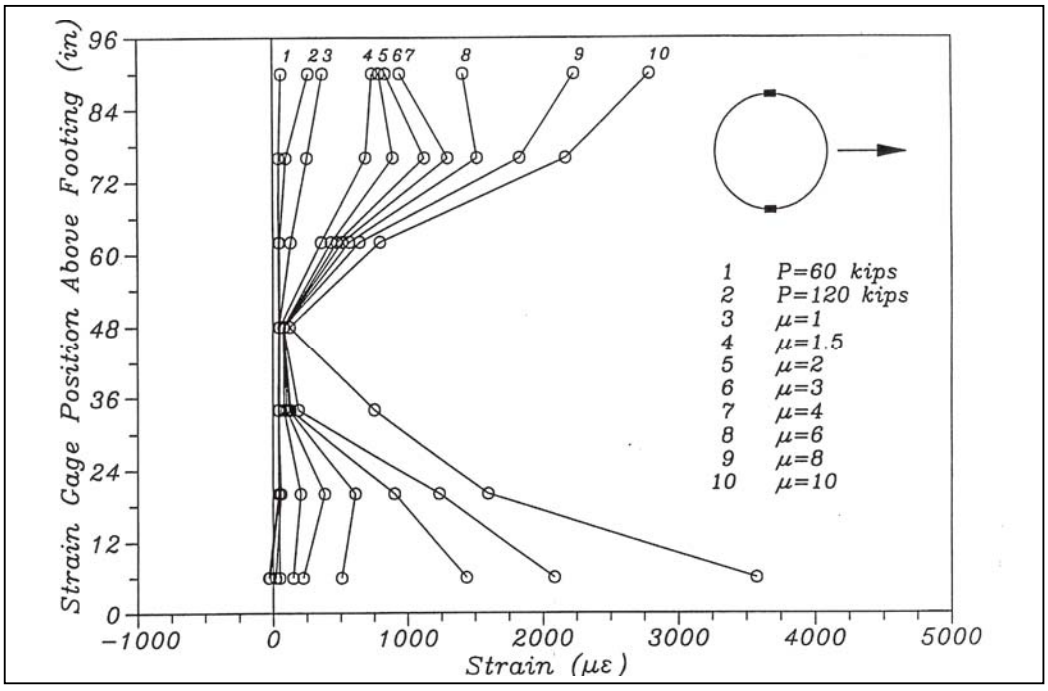

Figure D-7: Strain Profiles for Average of East and West Sides Pull Direction

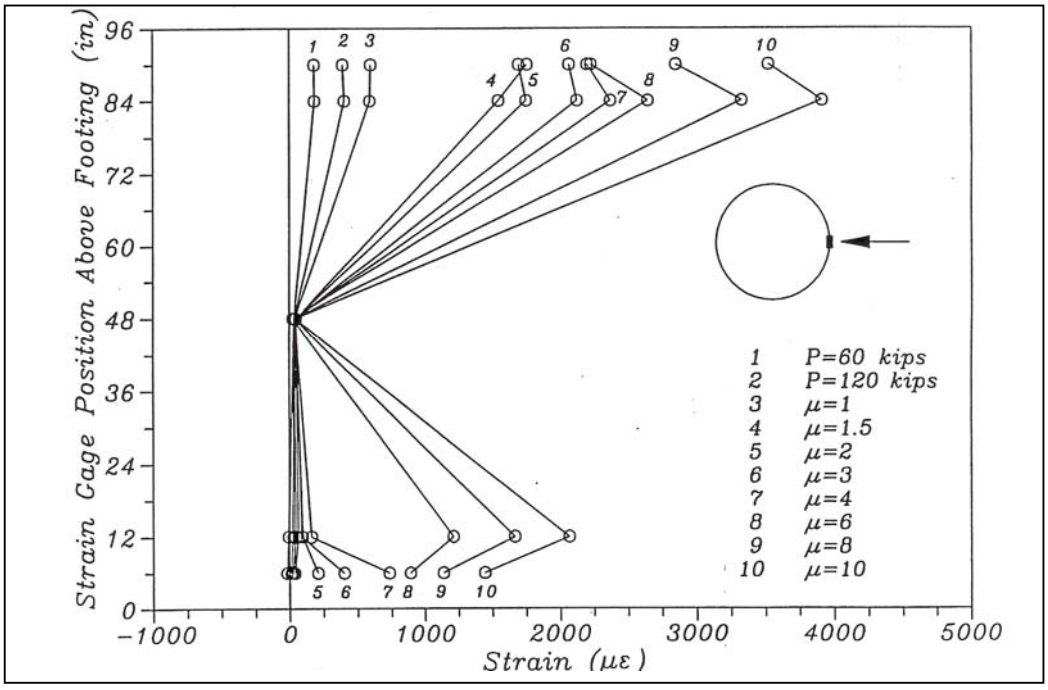

Figure D-8: Strain Profiles for North Side Push Direction

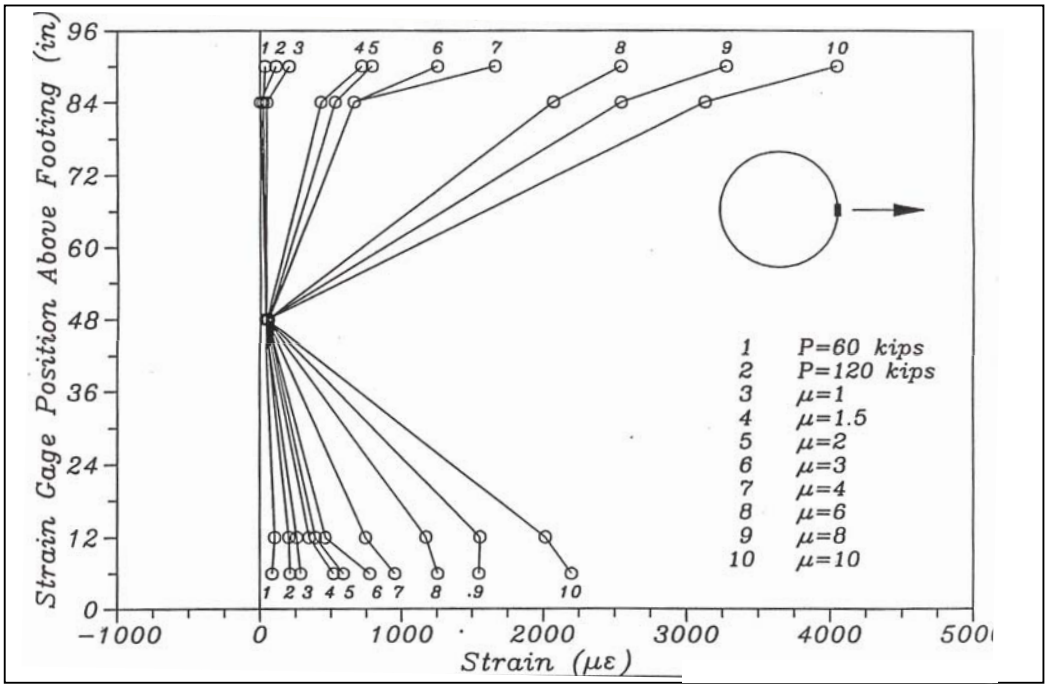

Figure D-9: Strain Profiles for North Side Pull Direction

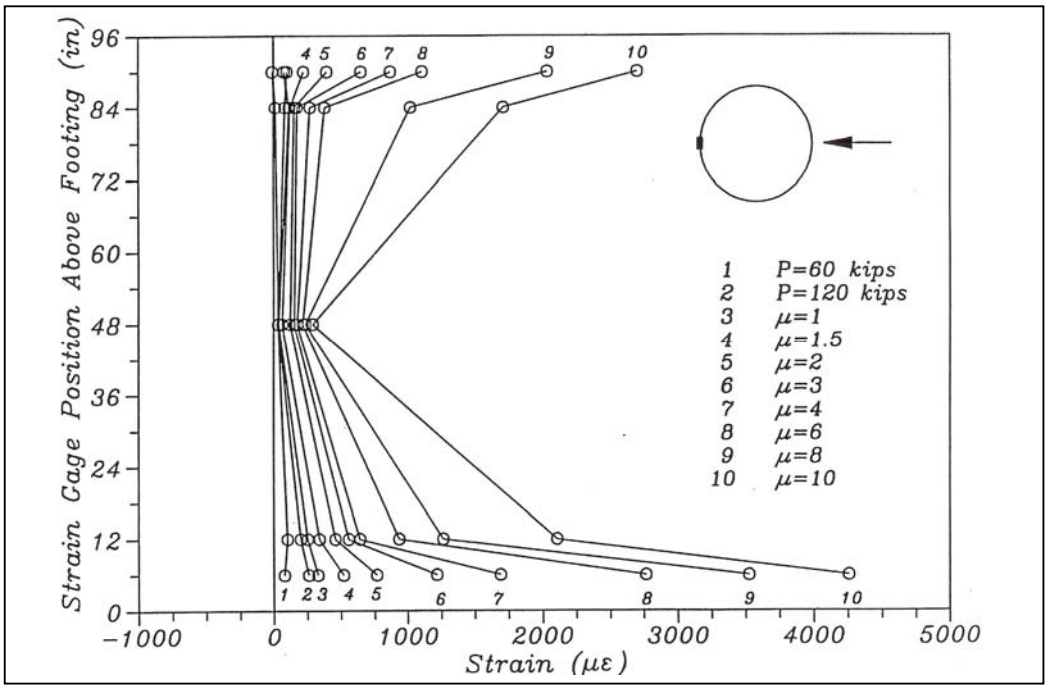

Figure D-10: Strain Profiles for South Side Push Direction

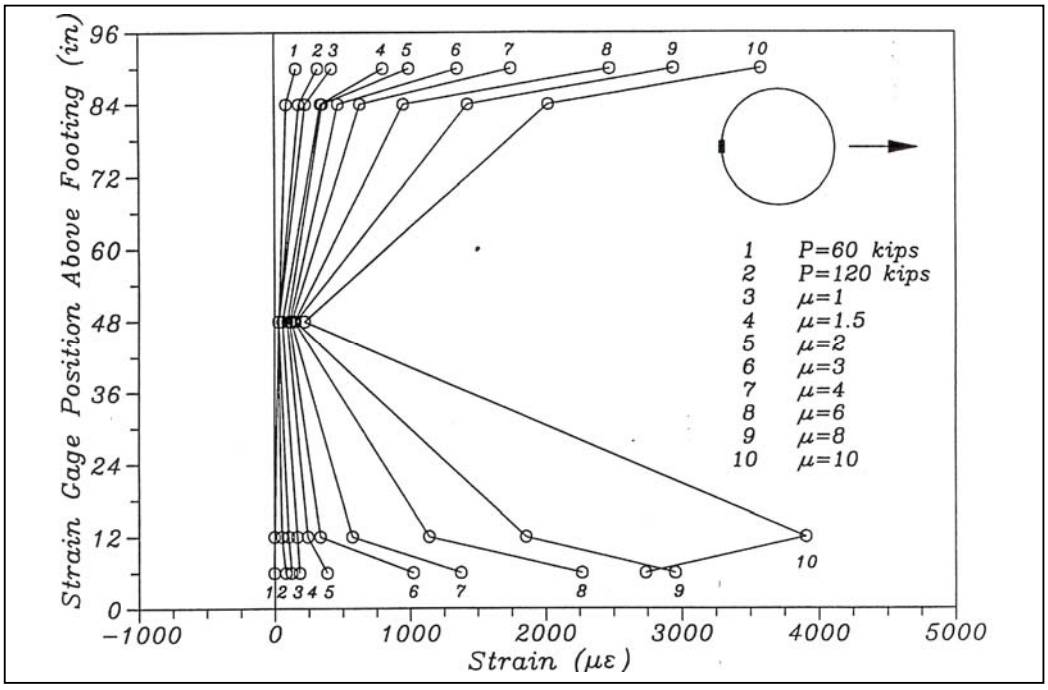

Figure D-11: Strain Profiles for South Side Pull Direction

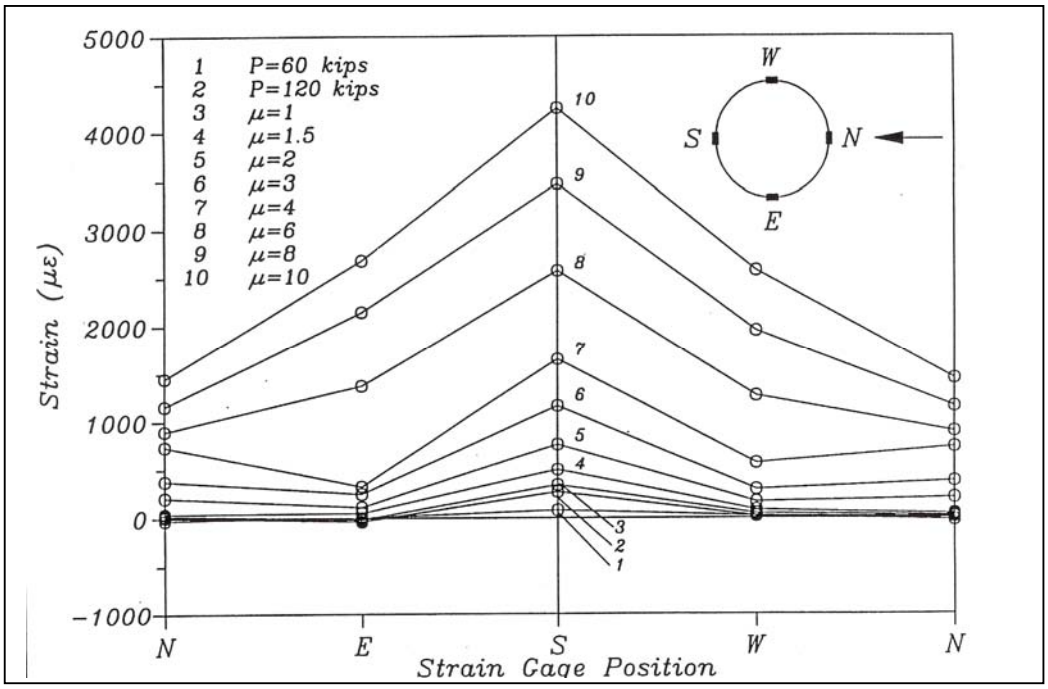

Figure D-12: Strain Profiles 6 Inches Up from Footing Push Direction

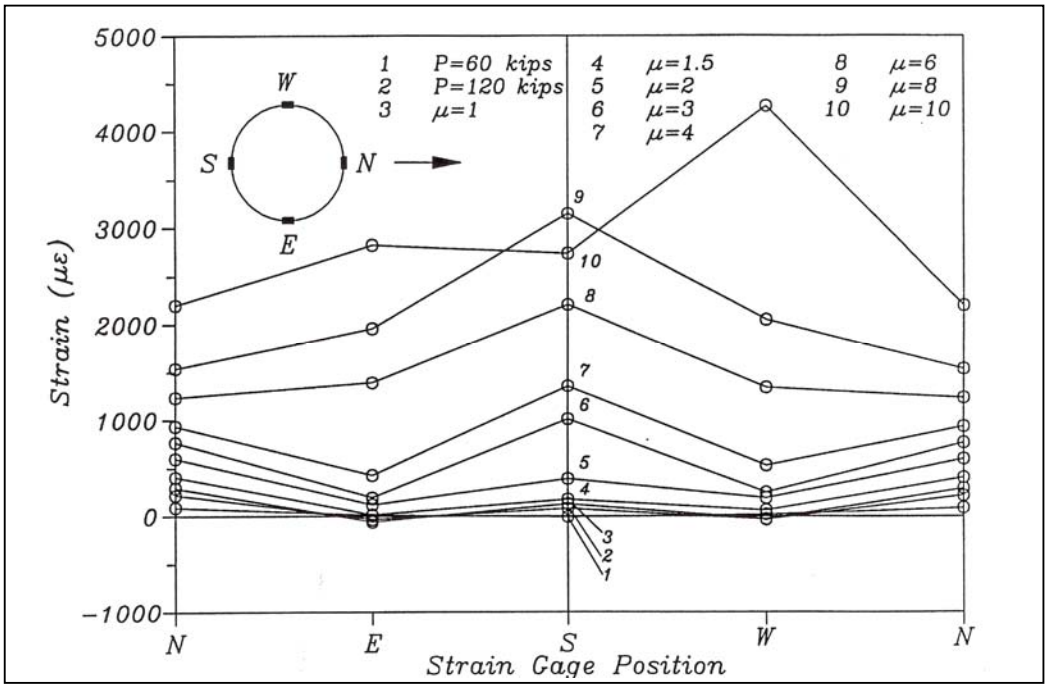

Figure D-13: Strain Profiles 6 Inches Up from Footing Pull Direction

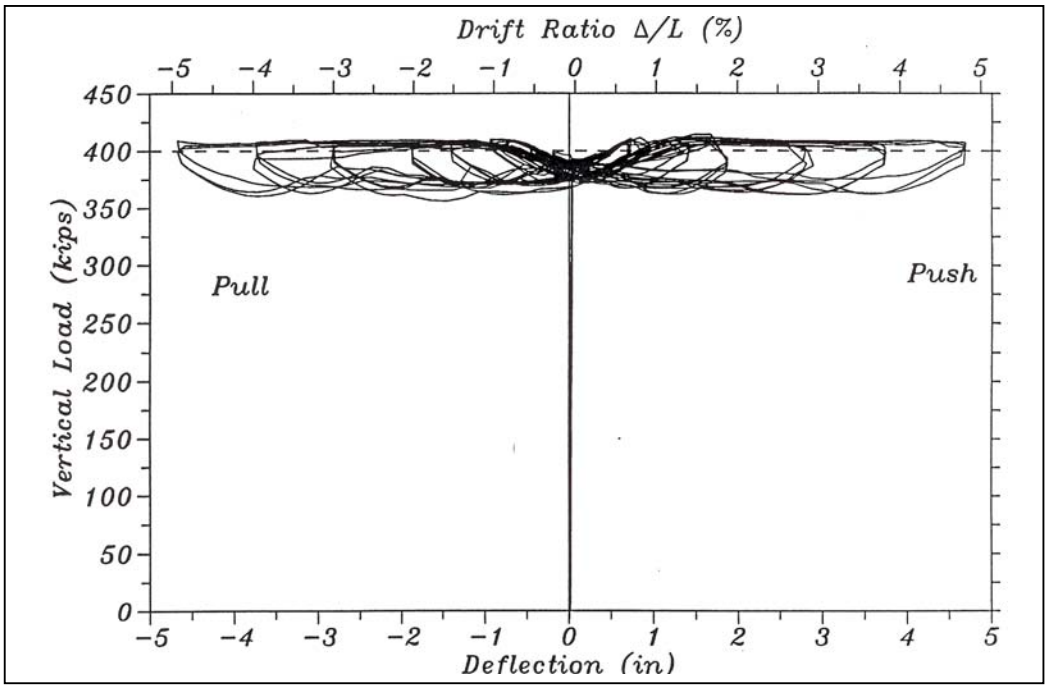

Figure D-14: Vertical Load vs Horizontal Deflection for Fibre Repaired Circular Shear Column